RAPID COMMUNICATIONS

PHYSICAL REVIEW B VOLUME 52, NUMBER 2 1 JULY 1995-II

Observation of below-gap plasmon excitations in superconducting $YBa_2Cu_3O_7$ films

F. J. Dunmore, D. Z. Liu,* H. D. Drew, and S. Das Sarma
Center for Superconductivity Research, Department of Physics, University of Maryland, College Park, Maryland 20742 and Laboratory for Physical Sciences, College Park, Maryland 20740

Qi Li and D. B. Fenner
Advanced Fuel Research Inc., East Hartford, Connecticut 06138
(Received 13 March 1995)

Finite-wave-vector collective plasmon resonances have been observed in far-infrared transmission measurements on superconducting $YBa_2Cu_3O_7$ films. An Al grating is used to couple IR radiation to collective two-dimensional plasma modes. The plasmon dispersion, measured by using different grating periods, spans the frequency range of the energy gap. The strengths of the plasma resonances weaken as the temperature approaches T_c from below. The results are analyzed using a grating coupler theory that includes the hybridization of the plasmons with the diffraction modes.

In the BCS theory of superconductivity the electrons condense into a collective ground state, which has an energy gap to quasiparticle excitations. However, the possibility of collective excitations with energies below the superconducting energy gap is not precluded. Recently, resonances in far-infrared response have been reported in $YBa_2Cu_3O_7$ (YBCO) which are related to the collective cyclotron resonance of the superconducting condensate.[1,2] Cyclotron resonance is a collective excitation corresponding to the center-of-mass cyclotron motion of the electron system. Also, a plasma edge has been observed in the c-axis far-infrared reflectivity spectrum in superconducting $La_{2-x}Sr_xCuO_4$.[3] This observation suggests the possibility of charge-density excitations existing below the energy gap. Very recently, dimensional plasma resonances [two-dimensional (2D) plasmons] have been reported at frequencies below the gap frequency $2\Delta=3.5kT_c$ in superconducting Al thin films in the GHz range.[4] These are long-wavelength plasmon excitations with wave vectors in the mm^{-1} range. In this paper we report the observation of 2D plasmon excitations in the superconducting state of YBCO with wave vectors in the μm^{-1} range. This is the first observation of plasmons in high-T_c superconductors. We also obtain the wave-vector dispersion of the plasmon mode in our experiment.

The possibility of observing a two-dimensional plasmon in the layered cuprate superconductors was predicted by Fertig and Das Sarma.[5] They proposed the possibility of the observation of a plasmon by near normal incident Raman spectroscopy on single crystals, where the strength of the plasmon with charge-density oscillation in the copper-oxygen planes would be limited by interplane tunneling in the superconducting state. The cuprates have a sufficiently small plasma frequency and large energy gap that two-dimensional plasmons may exist in thin films for reasonable thicknesses. Unlike three-dimensional plasmons, in which the dispersion is nearly independent of wave vector and nonzero at zero wave vector, the two-dimensional plasmon should have a wave-vector-dependent dispersion relation, with plasma frequency directly proportional to $q^{1/2}$. It is these two-dimensional plasmons that we study this work using a grating coupler to provide the in-plane wave vector.

The grating coupler technique has been extensively used to study collective modes in (nonsuperconducting) two-dimensional electron gas (2DEG) systems in Si metal-oxide-semiconductor structures, and GaAs/AlAs heterostructures and quantum wells.[6–8] For a 2DEG on a substrate of dielectric constant ε_s, with a complex frequency-dependent two-dimensional Drude conductivity $\sigma^{(2D)}(\omega)$, and a metallic grating with period a at a distance d above the 2DEG (separated by a layer with $\varepsilon=\varepsilon_0$), it can be shown that there is a pole in the effective grating/2DEG conductivity which gives rise to a minimum for the far-infrared transmission spectra.[9] In the $\lambda \gg d \gg a$ limit, the frequencies of these poles are given by the two-dimensional plasmon dispersion relation:[9]

$$\omega_{p,2D}=\left(\frac{4\pi n_{2D}e^2q}{m^*[\varepsilon_s+\varepsilon_0\coth(qd)]}\right)^{1/2}, \tag{1}$$

where $q=G_n=2\pi n/a$, $n=1,2,3,\ldots$ is the wave vector created by the grating where n_{2D} is the 2D charge density, and m^* is the effective mass in a lossless 2DEG conductivity of $\sigma^{(2D)}(\omega)=in_{2D}e^2/m^*\omega$. Since the London model for superconductors is equivalent to the lossless free-electron model at $q=0$ we might expect such plasmons to be observable in superconductors. For high-T_c superconductive films of useful thickness, however, the 2D carrier density is over two orders of magnitude higher than that in a 2DEG, and so the wavelength of light that can excite the collective modes is comparable to the grating period. Therefore it is necessary to accurately account for the coupling of the plasmon modes to the diffraction modes of the grating, which is not treated in the standard grating coupler theory of Ref. 9, where the long-wavelength regime was investigated theoretically.

We now briefly outline our theory of a grating coupler near the diffraction limit.[10] As in Ref. 9 we calculate the experimentally measurable transmission amplitude of a zero-order light beam through the grating (at $x=0$) and superconductive thin film (at $x=d$), on a substrate of dielectric constant ε_s, separated by a dielectric spacer layer of dielectric constant ε_0, each having a corresponding zero-order conductivity $\Sigma^{(g)}(\omega)$ and $\sigma^{(s)}(\omega)$ in the y-z plane. We evaluate the zero-order grating conductivity $\Sigma^{(g)}(\omega)$ by analyzing the

higher-order local field generated by the grating coupler. When the wavelength of the infrared light is comparable to the grating period, it is necessary to consider the local magnetic field: $\mathbf{B}_L = -ic/\omega \nabla \times \mathbf{E}_L$. By applying the boundary conditions $\Delta \mathbf{E}_L = \mathbf{0}$ and $\mathbf{e}_x \cdot \mathbf{D}_L = 4\pi \nabla \cdot \mathbf{J}/i\omega$ at $x=0$ and d, we can get an equation for the nth-order conductivitylike function of the grating, F_n, as defined by Zheng *et al.*:[9]

$$F_n = \frac{i\omega}{4\pi H_n}\left[1+\varepsilon_0\frac{H_n}{I_n}\coth(I_n d) + \frac{\varepsilon_0^2\frac{H_n J_n}{I_n^2}(1-\coth^2(I_n d))}{i\frac{4\pi}{\omega}J_n\sigma_{yy}^{(s)}(\omega,G_n)+\varepsilon_s+\varepsilon_0\frac{J_n}{I_n}\coth(I_n d)}\right]. \quad (2)$$

This function is used in conjunction with the Fourier components of the grating resistivity to iteratively calculate the effective grating conductivity $\Sigma^{(g)}(\omega)$. Here $G_n = 2\pi n/a$, $n=1,2,3,\ldots$ is the grating spatial frequency. $H_n = (G_n^2 - \omega^2/c^2)^{1/2}$, $I_n = (G_n^2 - \varepsilon_0\omega^2/c^2)^{1/2}$, and $J_n = (G_n^2 - \varepsilon_s\omega^2/c^2)^{1/2}$ replace G_n in Eqs. (18) and (23) of Zheng *et al.*[9] for $x<0$, $0<x<d$, and $d<x$, respectively. When $\sqrt{\varepsilon_s}\omega/c \geq G_n$, J_n becomes imaginary and the otherwise evanescent local field begins to propagate, becoming the higher-order diffracted beam, and removes intensity from the zero-order beam. $\sigma_{yy}^{(s)}(\omega, q=G_n)$ is the frequency and momentum dependent two-dimensional conductivity tensor component of the YBCO thin film for the direction perpendicular to the grating. For YBCO both ξ^{-1}, the inverse coherence length, and k_F, the Fermi wave vector, $\cong 10^7$ cm^{-1}, are large compared to $G_n \cong 10^4$ cm^{-1}, and therefore $\sigma_{yy}^{(s)}(\omega, q=G_n)$ is expected to be practically independent of wave vector within the experimental wave-vector range reported here. Therefore the conductivity for the YBCO thin film is assumed to be $\sigma_{yy}^{(s)}(\omega, q=0)$ for all calculations. However, the grating conductivity is still strongly affected by the YBCO thin film.

In the $\lambda \gg d \gg a$ limit the minima in the transmission spectrum are determined by the poles of the grating's conductivitylike F_n functions. These poles are determined by the zero of the denominator of the last term in the square brackets in Eq. (2). The dispersion relation of these poles reduces to Eq. (1) if $G_n \gg \omega/c$ and the quasiparticle lifetime is infinite. This pole in F_n produces a nearby zero in the imaginary part of the total effective conductivity, $\sigma^{(s)}(\omega) + \Sigma^{(g)}(\omega)$, which leads to a transmission maximum at a frequency below that of the transmission minimum. We will refer to this feature as the plasmon antiresonance. The expression for transmission and reflection are discussed in detail in Ref. 9. In our calculations we have made corrections for multiple internal reflections in the substrate. The finite thickness of the YBCO, yttrium stabilized zirconia (YSZ), and polymethylmethacrylate (PMMA) layers and the phases of the incident field at the boundaries have been taken into account in all of our calculations. The differences between the thin film approximation and the full finite layer transmission are small, so that the thin film model is an excellent approximation.

Sample 1 is a 400 Å film with T_c of 88 K with a 2 K linewidth, grown by laser ablation on Si substrate, with a YSZ cap and buffer layers of thickness 500–600 Å. Sample 2 is the same but with a 200 Å YBCO film. The details of the growth process are given elsewhere.[11] Grating couplers of aluminum, for the low-resistivity (~1 Ω/□) part of the grating, and nichrome, for the high-resistivity (several kΩ/□) part, with periods ranging from 5 to 25 μm, were fabricated using photolithographic processing. A 1500–2000 Å PMMA dielectric spacer layer of dielectric constant $\varepsilon_0 = 3.0$ between sample and grating controls the coupling strength between the plasma modes and the electric field of the incident radiation. The sample geometry is shown schematically in the inset of Fig. 1. After the first grating application the critical temperatures of both samples dropped to 75 K and the transition widths increased to 10 K. We attribute this change in T_c to oxygen depletion at the YBCO/YSZ boundaries during the 160 K PMMA heat curing process. The YBCO films still exhibited London behavior at low frequencies and low temperatures.

We measured the transmission ratio T_r of the grating/YBCO/Si sample relative to that of a bare Si substrate reference. The sample and a Si reference were cooled together to $T \geq 10$ K in a separate optical transmission Dewar where they could be switched *in situ* into and out of the path of the IR beam. The transmission was measured using a rapid scan Fourier transform spectrometer with a Hg vapor lamp source. A 4 K Si bolometer detector was used for the sample 1 measurements in the frequency range 50 cm$^{-1} \leq \omega \leq 700$ cm^{-1}. A Si bolometer detector cooled to 1.5 K was used for sample

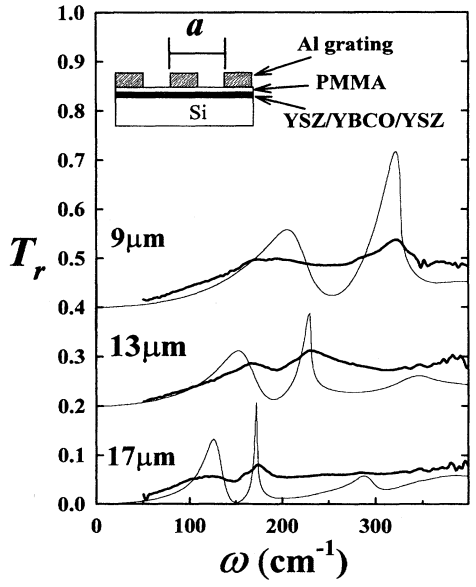

FIG. 1. The transmission ratios for three selected grating periods are plotted along with theoretical predictions. The curves are shifted on the T_r axis for clarity. At the top curve is the 9 μm grating data, the middle is 13 μm, and the bottom is 17 μm. As the grating period increases from 9 to 17 μm, the frequency position of the plasmon decreases roughly as the square root of q. The inset figure is a schematic of the sample, with grating period a.

2 in the frequency range 30 $cm^{-1} \leq \omega \leq 200$ cm^{-1}. Sample 1 had 5, 7, 9, 11, 13, and 17 μm gratings; sample 2 had a 25 μm period grating.

The YBCO samples were first optically characterized without a grating. A two-component London-Drude model describes the YBCO complex conductivity $\sigma^{(s)}(\omega)=(\omega_p^2/4\pi)\mathcal{F}$, where $\mathcal{F}=i(f_s/\omega+f_n/\tilde{\omega})$ with $\tilde{\omega}=\omega+i\tau^{-1}$. Here f_s describes the superfluid (London) fraction and f_n describes the lossy component, which we model as a zero-frequency oscillator of the Drude form. This component may come from weak links or nonsuperconducting layers in the film. The oscillator strength sum rule requires that $f_s+f_n=1$, $\omega_p=(4\pi Ne^2/m^*)^{1/2}$ is the three-dimensional plasma frequency, and τ the normal-state quasiparticle lifetime. A Lorentzian term describing the mid-infrared frequency response of the chains was also included to fit the high-frequency part of the transmission of the bare film.[12] The transmission ratio of the YBCO film/substrate sample to the bare substrate reference is given by $T_r \cong 1/|1+y|^2$ with $y=\Omega\mathcal{F}$ where $\Omega=\omega_p^2 d_f/(n_{Si}+1)c$ is the width of the Lorentzian transmission line shape, d_f is the YBCO film thickness, and $n_{Si} \equiv \sqrt{\varepsilon_s}=3.4$ is the index of refraction for the silicon substrate. The low-frequency London penetration depth λ_L is given by $\lambda_L^2=c^2/f_s\omega_p^2$. The parameter Ω was fit to an uncertainty of $\pm 10\%$ from the transmission ratio of the bare sample, with similar uncertainty for f_s, and τ.

In Fig. 1 the measured transmission ratios for three selected grating periods are shown along with their calculated theoretical representations from the London-Drude model. The transmission for both samples was found to have London behavior ($T_r \to 0$ as $\omega \to 0$) at low frequency both with and without a grating. The frequency of the plasmon resonance is the pole of the effective conductivity of the YBCO-grating system, given approximately by Eq. (1). The dispersion is sensitive not only to the grating period, but also to the spacing between the grating and the YBCO layer. The spacer distance is $d=0.16$–0.17 μm; the YBCO film parameters for sample 1 are $\Omega=550$ cm^{-1}, $f_s=0.8$, $1/\tau=130$ cm^{-1}. For the 9 μm data T_r increases from zero frequency roughly linearly to a maximum around 200 cm^{-1}. Then T_r decreases to a minimum at 250 cm^{-1}, then increases to a larger and sharper maximum at 320 cm^{-1}. Finally T_r gradually decreases, flattening out beyond 400 cm^{-1}. The first peak is the plasmon antiresonance which is due to a zero-crossing in the imaginary part of the total effective conductivity, the dip is due to the plasma resonance and the second peak is due to diffraction from the grating. The calculated frequency positions of the plasmon and the diffraction peaks from the calculation agree well with the data. The calculation gives sharper features than those found in the experiments. Grating defects and nonuniformity of the resistivity of the high-resistivity nichrome part of the grating as well as low-frequency PMMA losses are the probable causes for the extra broadening of the resonances. One can easily account for this in the theory by introducing an additional phenomenological broadening parameter.[10]

The width of the plasmon minimum and the diffraction peak get narrower for the lower q gratings indicative of reduced dissipation at lower frequencies. As the grating period increases from 9 to 13 to 17 μm, the frequency position of the plasmon decreases roughly as $q^{1/2}$. At frequencies above the diffraction frequency, we believe the diffracted light is recaptured by the optics and its detection, not included in the theory, leading to higher apparent transmission than the calculations. The qualitative agreement between the data curves and the calculations and the quantitative agreement between the two in terms of the frequency position of the diffraction peak and the plasma resonance minimum imply that we are observing a plasma resonance in the YBCO.

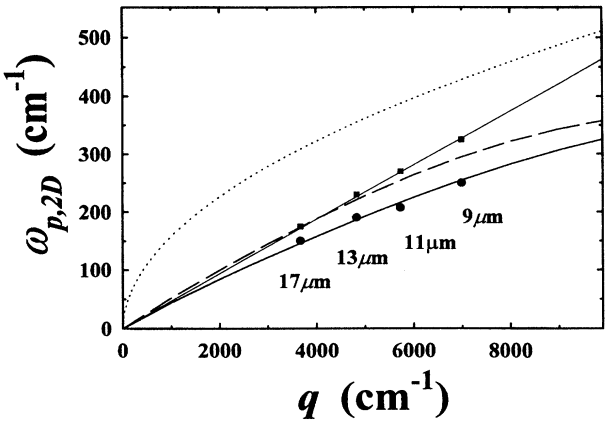

FIG. 2. The curved solid line is the plasmon dispersion relation for the parameters fitting the 400 Å sample compared to the data shown as the circular dots which are the plasma resonance frequencies versus the q of the corresponding grating. The curved-dashed line is for the $\lambda \gg a$ theory. The straight solid line is the diffraction frequency of a grating as a function of q. The squares are the data's diffraction peak frequencies. The curved-dotted line is the plasmon dispersion relation for the infinite-wavelength theory with an infinite distance between the grating and the YBCO.

In Fig. 2 the dispersion relation for sample 1 is shown in comparison to the calculated result using the YBCO conductivity described by parameters fitting the London-Drude model as discussed previously. The uncertainty for the data points approximately equal their dimensions on the graph. Both our finite-wavelength calculation and the $\lambda \gg a$ theory of Ref. 9 are shown. Shown in addition is the $\lambda \gg d \gg a$ limit of the plasmon dispersion relation in which the interaction of the YBCO thin film with the grating is negligible.[9] The plasmon data points agree well with our $\lambda \cong a$ theory. This shows that our theory is appropriate for the finite-wavelength regime.

In the top panel of Fig. 3 the transmission ratio of the 25 μm grating coupled sample 2 is shown as a function of temperature. The antiresonance peak around 70 cm^{-1} has maximum amplitude at 10 K and reaches minimum amplitude at 70 K near T_c. The local minimum in T_r at 90 cm^{-1} at the plasma resonance increases in magnitude as the temperature increases, indicative of less screening of the incident electric field as the superfluid fraction decreases. The diffraction peak at 117 cm^{-1} decreases in magnitude and broadens as the temperature increases, indicative of increasing dissipation. Most importantly the plasma resonance disappears around $T \cong T_c$. Therefore we infer that it is the superfluid condensate that is producing the main plasmon response, and it is the lossy nature of the normal state that damps the plas-

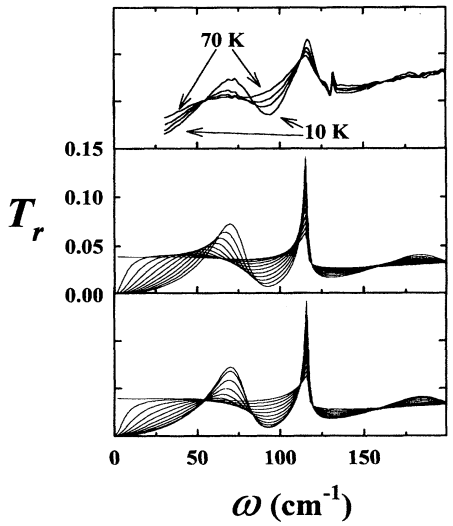

FIG. 3. Top panel: the transmission ratio for the 200 Å sample with a 25 μm grating at 10, 50, 60, and 70 K. Middle panel: the calculations where the scattering rate is a constant; the frequency position of the antiresonance peak decreases rapidly as the normal-state fraction increases, unlike the data. Bottom panel: the calculated transmission for a two-fluid model for the condensable component, where the scattering rate is directly proportional to the normal-state fraction.

mon making it unobservable above T_c. The calculations shown in the bottom two panels of Fig. 3 are based on a two-component London-Drude model with parameters $\Omega = 360$ cm^{-1}, $f_s = 0.7$, and $1/\tau = 115$ cm^{-1} at 10 K.

The middle panel of Fig. 3 shows the results of T_r calculations for the case when the scattering rate is a constant. The antiresonance peak's frequency position rapidly decreases as the normal-state fraction increases, unlike the experimental data. The bottom panel of Fig. 3 shows the T_r calculations for a model where we treated the lossy component of the fit at 10 K as uncondensable, and the remaining component as a condensible superfluid at low temperature which we treat in the two fluid model. We have set the scattering rate of the normal-state fraction of this condensable component directly proportional to that fraction in the spirit of quasiparticle-quasiparticle scattering arguments used to interpret the recent microwave quasiparticle lifetime measurements in YBCO crystals.[13–15] A more refined model including the temperature and frequency dependence of the quasiparticle scattering rate is not warranted at this point. To illustrate the results of this model we have varied the normal-state fraction from 0 to 1 in 0.1 increments corresponding to the temperature increasing from 0 K to T_c. It is seen that the position of the antiresonance peak remains nearly constant for normal-state fractions less than 0.4 in the calculations compared with $T \leq 60$ K observed in the measurements. The calculations also produce the small downward shifts observed in the experiments as the temperature is raised above 60 K.

The better agreement of the data with a model where the scattering rate is proportional to the normal-state quasiparticle density is evidence that the scattering rate is suppressed at low quasiparticle densities, similar to the results of other experiments on the cuprates. This has been pointed to as evidence for strong electron-electron interaction between normal-state quasiparticles, and is predicted by various nonphonon-mediated theoretical approaches to high-T_c superconductivity such as spin-fluctuation coupling and marginal Fermi-liquid related theories. A recent theoretical analysis[16] shows, however, that for the wave-vector range of our experiment the plasmon dispersion is independent of the ground-state symmetry (s- or d-wave) of the superconducting state, and, therefore, our work does not distinguish between the s- or d-wave nature of the YBCO ground state.

In summary, we have measured the far-infrared transmission of YBCO with a photolithographically defined Al grating coupler and have found plasma resonance-related features whose frequency positions are accurately predicted by a finite-wave-vector theory of two-dimensional grating coupled plasmons. The data are characteristic of a plasma resonance in the superfluid which disappears as the temperature reaches the critical temperature. The data are also consistent with the normal-state quasiparticle lifetime being inversely proportional to the quasiparticle density, in agreement with other measurements on the cuprates.

We gratefully acknowledge helpful discussions with E. J. Nicol, David Evans, Geoffrey Burge, David Rush, Jaspal Singh, P. T. Ho, Chia-Hung Yuang, D. Song, Shaohua Liu, and Khaled Karraï. This work is supported by the NSF (F.J.D. and H.D.D.), by the NSF and the U.S.-O.N.R. (D.Z.L. and S.D.D.), and by the BMDO-AFOSR, Grant No. F49620-93-C-0010 (Qi Li and D.B.F.).

*Present address: James Franck Institute, University of Chicago, Chicago, IL 60637.

[1] K. Karraï *et al.*, Phys. Rev. Lett. **69**, 152 (1992).
[2] K. Karraï *et al.*, Phys. Rev. Lett. **69**, 355 (1992).
[3] K. Tamasaku, Y. Nakamura, and S. Uchida, Phys. Rev. Lett. **69**, 1455 (1992).
[4] O. Buisson, P. Xavier, and J. Richard, Phys. Rev. Lett. **73**, 3153 (1994).
[5] H. A. Fertig and S. Das Sarma, Phys. Rev. Lett. **65**, 1482 (1990); Phys. Rev. B **44**, 4480 (1991).
[6] E. Batke, D. Heitmann, and C. W. Tu, Phys. Rev. B **34**, 6951 (1986).
[7] S. J. Allen, Jr., D. C. Tsui, and R. A. Logan, Phys. Rev. Lett. **38**, 980 (1977).
[8] D. Heitmann and U. Mackens, Phys. Rev. B **33**, 8269 (1986).
[9] Lian Zheng, W. L. Schiach, and A. H. MacDonald, Phys Rev. B **41**, 8493 (1990); D. Z. Liu and S. Das Sarma, Phys. Rev. B **44**, 9122 (1991).
[10] Further details are in F. J. Dunmore (unpublished).
[11] D. K. Fork *et al.*, Appl. Phys. Lett. **57**, 1161 (1990); **57**, 1137 (1990).
[12] D. B. Tanner and T. Timusk, in *Properties of High Temperature Superconductors*, edited by D. M. Ginsberg (World Scientific, Singapore, 1987).
[13] D. A. Bonn *et al.*, Phys. Rev. Lett. **68**, 2390 (1992).
[14] L. Forro *et al.*, Phys. Rev. Lett. **65**, 1941 (1990).
[15] R. T. Collins *et al.*, Phys. Rev. B **43**, 8701 (1991).
[16] E. H. Hwang and S. Das Sarma (unpublished).